

# PREPARATION OF POLY(GLYCEROL SEBACATE) FIBERS FOR TISSUE ENGINEERING APPLICATIONS

Merve Gultekinoglu<sup>a,b</sup>, Şükrü Öztürk<sup>a,b</sup>, Biqiong Chen<sup>c</sup>,

Mohan Edirisinghe<sup>d\*</sup>, Kezban Ulubayram<sup>a,b,e,f\*</sup>

<sup>a</sup> Department of Basic Pharmaceutical Sciences, Faculty of Pharmacy, Hacettepe University, Ankara 06100, Turkey,

<sup>b</sup> Bioengineering Division, Institute for Graduate Studies in Science and Engineering, Hacettepe University, Ankara 06640, Turkey,

<sup>c</sup> School of Mechanical and Aerospace Engineering, Queen's University Belfast, Stranmillis Road, Belfast BT9 5AH, UK

<sup>d</sup> Department of Mechanical Engineering, University College London (UCL), London WC1E 7JE, UK

<sup>e</sup> Nanotechnology and Nanomedicine Division, Institute for Graduate Studies in Science & Engineering, Hacettepe University, Ankara 06640, Turkey

<sup>f</sup> Polymer Science and Technology Division, Institute for Graduate Studies in Science & Engineering, Hacettepe University, Ankara 06640, Turkey

- Co-corresponding author: m.edirisinghe@ucl.ac.uk, ukezban@hacettepe.edu.tr

## **ABSTRACT**

Poly(glycerol sebacate) (PGS) was discovered in the previous decade and is a promising bioelastomer with tuneable mechanical, biodegradable and biocompatible properties. Despite of these superiorities, PGS possesses solubility and processability disadvantages. To overcome these drawbacks of PGS, blends could be formed with a polymer which is soluble in a common solvent with PGS prepolymer, having a melting temperature above the crosslinking temperature and which can be removed from the structure after crosslinking. In this study, PGS fibers were fabricated for the first time using pressurized gyration as scaffolds. Fibers were obtained through blending the synthesized PGS prepolymer with poly(vinyl alcohol) (PVA) to overcome solubility/melting drawbacks of crosslinked PGS polymer. Obtained fiber diameters have a narrow size distribution which did not change after thermal crosslinking. After the washing procedure, ~ 25% decrease in the average fiber diameter was observed due to the PVA removal. Resulting PGS fibers were characterized in terms of chemical structure, morphology, and cell viability. Fibroblast cell adhesion and spreading on three-dimensional fiber networks were determined by microscopy. PGS fibers supported cell adhesion and proliferation. After 7 days of cell-PGS fiber interactions, cell proliferation and spreading increased without any toxicity.

**Keywords:** Poly(glycerol sebacate) (PGS), pressurized gyration, fiber, scaffold.

## 1. Introduction

Poly (glycerol sebacate) (PGS), has become a promising polymer for tissue engineering applications, especially in soft tissue applications such as cardiac [1], nerve [2], blood vessels [3], cornea [4] tissue engineering etc., due to its elastomeric, mechanical and biocompatible properties. Also, PGS possesses the advantages of tuneable biodegradable properties that become effective enzymatically and hydrolytically without any toxic effects of degradation products. The major drawback of PGS is the process difficulty resulting of low solubility, especially after thermal crosslinking. PGS scaffolds can be produced with the prepolymer, but the resulting structure then melts in the thermal crosslinking step and loses its well defined shape. In addition to that, porogen leaching after crosslinking is an approach for the fabrication of porous scaffolds, however pore shape and interconnectivity of scaffolds produced by this method is not controllable. To overcome this limitation, blends could be formed with other polymers which are soluble in a common solvent with PGS prepolymer, having a melting temperature above the crosslinking temperature. Therefore, there are several studies using PGS-based blends and/or copolymer structures to diversify the area of use [5-8]. As it is well known that the use of fiber scaffolds for tissue regeneration is advantageous due to their extracellular matrix (ECM) mimicking properties. However, the preparation of PGS scaffolds as fiber form is limited for tissue engineering applications due to low process ability of polymer. Hence, viscous spinning solutions can be obtained by blending PGS with other polymers and these solutions can be further spun into non-woven fibrous scaffolds. Blends of PGS with various synthetic polymers (i.e. poly(vinyl alcohol) (PVA), poly(ethylene oxide), poly(hydroxy butyrate), poly ( $\epsilon$ -caprolactone)) were electrospun to obtain fibrous scaffolds

and exhibited promising results to be used in several tissue types such as retinal, dermal and vascular [9-11].

Non-nozzle fiber preparation techniques have been developed in the last decade and these do not require an electrical potential difference in the spinning processes and allow the formation of fiber with the help of centrifugal force. The obtained fibers have been studied in various applications from energy storage to tissue engineering [12-14]. Electrohydrodynamic (EHD) spinning is also very frequently used technique particularly in tissue engineering applications [15-18]. However, it has been reported that the fibers are produced with much higher yield by the centrifugal spinning compared to the EHD spinning [19]. Pressurized gyration, also referred to as gyrospinning, uses high-speed rotation (centrifugal force) and pressure together to generate multiple solution jets radially from holes in the surface of the rotary cuvette [20]. A container made of cylindrical and aluminium metal can rotate around its axis with the aid of an electric motor and the gas inlet is provided by an inlet on the top of the container. There are micrometer size holes on the metal container that allow the release of the polymer solution. In a typical procedure, batch production is carried out and the previously prepared polymer solution is pre-added in the container. As the container rotates, the polymer jet emerges from the holes to form the fibers. The most important advantage of the pressurized gyration technique, as against the electrospinning, is that it does not pose any restrictions on electrical properties such as electrical conductivity and dielectric constant for fiber preparation [19, 21]. This advantage therefore eliminates the limitation of the use of non-conductive solutions encountered in electrospinning. Physical properties such as diameter distribution, homogeneity in morphology, and fiber structure produced by

pressurized junction are related to preparation (rotation speed, pressure and order of collection elements) parameters [22]. There have been several studies with pressurized gyration which include drug-releasing fibers, scaffolds for tissue engineering, and micro bubbles for diagnostic applications [23-25]. In the literature, synthetic polymers such as poly(ethylene terephthalate), poly(acrylonitrile), poly(methyl methacrylate), poly(ethylene oxide) and poly(vinyl pyrrolidone) as well as natural polymers such as sodium alginate, starch and carboxy methyl cellulose have been used in the preparation of micro/nano fibers by the pressurized gyration technique [20, 22, 26-28]. The reasons for using fibers produced by pressurized gyration in tissue engineering applications are mainly driven by the fact that the fibres can be generated in a highly oriented manner with high surface area/volume ratio.

In the present study, PGS fibers were formed by pressurised gyration and assessed for tissue engineering applications. For this purpose, PGS prepolymers were synthesized and blended with different molecular weights of PVA to overcome solubility/melting drawbacks of crosslinked PGS polymer. Subsequently, the polymer was gyrosun into fibers which were thermally crosslinked and blended PVA content was removed by washing procedure. Fiber forming conditions were optimised in terms of concentration, pressure and blended polymer content. Cytotoxicity evaluations of the polymer fiber were performed, cell viability and attachment evaluations were carried out by fluorescent cell staining experiments up to 7 days.

## 2. Materials and Methods

### 2.1. Materials

Sebacic acid (99%), glycerol bioXtra ( $\geq 99\%$ , GC), poly(vinyl alcohol) (PVA) Mw 89,000-98,000, 99+% hydrolysed, PVA Mw 30,000-70,000, 87-90% hydrolysed, PVA average Mw 146,000-186,000, 87-89% hydrolysed, glutaraldehyde, hexamethyldisilazane, dimethyl sulfoxide (DMSO) and 1,1,1,3,3,3-Hexafluoro-2-propanol  $\geq 99\%$  (HFIP) were obtained from Sigma-Aldrich and used directly. Phosphate buffer, DMEM (Dulbecco's Modified Eagle Medium), Fetal Bovine Serum (FBS), Penicillin/streptomycin, L-glutamine, MTT (4,5-Dimethylthiazol-2-yl)-2,5-diphenyltetrazolium bromide), Trypsin/Edta and LIVE/DEAD™ Viability/Cytotoxicity Kit, for mammalian cells were purchased from Biochrom, Germany.

### 2.2. Synthesis of Poly(glycerol sebacate) (PGS)

As illustrated in Figure 1A, PGS prepolymer (pPGS) was synthesized in house by rapid microwave-assisted polymerization [29]. The condensation reaction of equimolar glycerol and sebacic acid (1:1) was irradiated in microwave oven (Samsung, South Korea) for 3 minutes with 15 second intervals at 650 W.

### 2.3. Preparation of Gyrospun Solutions

Firstly, pPGS and PVA blends were dissolved in HFIP with 55:45-pPGS:PVA weight ratio and stirred overnight [30]. Three different molecular weights of PVA (Mw 30,000-70,000, 89,000-98,000 and 146,000-186,000) and 5, 10 and 15% (w/v) concentrations of pPGS:PVA blends were used. The viscosity of the solutions was determined using a Brookfield DV-III Ultra Viscometer (Brookfield Viscometers Ltd, Harlow, UK) with an

attached SCV-18 spindle. In addition, surface tension values were measured by a Krüss digital tensiometer K9 using the Standard Wilhelmy plate method.

#### 2.4. Preparation of PGS Fibers Using Pressurised Gyration

Pressurized gyration technique is schematically represented in Figure 1B. Basically, the experimental set-up contains rotary cylindrical aluminium vessel, gas inlet, rotary motor, speed and gas controllers in a safety cabinet. Aluminium vessel has dimensions ~ 60 mm diameter x 35 mm height and 24 orifices in the centre line with the 0.25 mm radius. In each batch, 5 mL polymer solution was placed in the vessel and gyrosun fibers were fabricated at optimized system parameters (36,000 rpm rotating speed and 0.1 MPa N<sub>2</sub>) at ambient conditions (45±5 % humidity and 24±2 °C temperature). After fiber forming, pPGS:PVA blend fibers were thermally crosslinked at 130 °C and 60 mm Hg for 48h. Subsequently, fibers were washed with deionized water for 24 h to remove the PVA from the gyrosun fibers and ethanol (serial dilutions 25, 50, 75 and 100% (v/v) ethanol/deionized water mixtures) to remove non-crosslinked pPGS residues.

#### 2.5. Characterization of PGS Polymer

Structural analysis of the synthesized polymer was carried out by <sup>1</sup>H-NMR analysis. The spectrum was recorded at 25 °C with a 400 MHz NMR (Bruker, Germany) spectrometer. Chemical characterization of the structures was carried out with a FTIR Spectrophotometer (Thermo Nicolet IS-50, Germany) with ATR attachment at a wavelength of 600-4000 cm<sup>-1</sup> and a resolution of 4 cm<sup>-1</sup> and 32 scans. The thermal stability of the synthesized polymer was evaluated with the TA Instruments Q600-SDT (USA) device at a heating rate of 10 °C/min in the range 25°C-600 °C in N<sub>2</sub> atmosphere at the 100 mL/min purge rate. The glass transition temperatures and energy capacities of

the synthesized polymer structure was carried out with a Differential Scanning Calorimeter (Perkin Elmer Diamond DSC, USA) at a heating rate of 10 °C/min in the range -60 °C-300 °C in N<sub>2</sub> atmosphere at the 50 mL/min purge rate. The mechanical properties of the synthesized polymer were carried out using a mechanical testing machine (Zwick / Roell Z250, Germany) in a conditioned environment of ~ 47% moisture and 24 °C temperature. The tensile speed was 10 mm/min and the tensile load was kept constant at 100 N. The Young's modulus value was calculated using the slope of the initial linear stress-strain curve (n = 3).

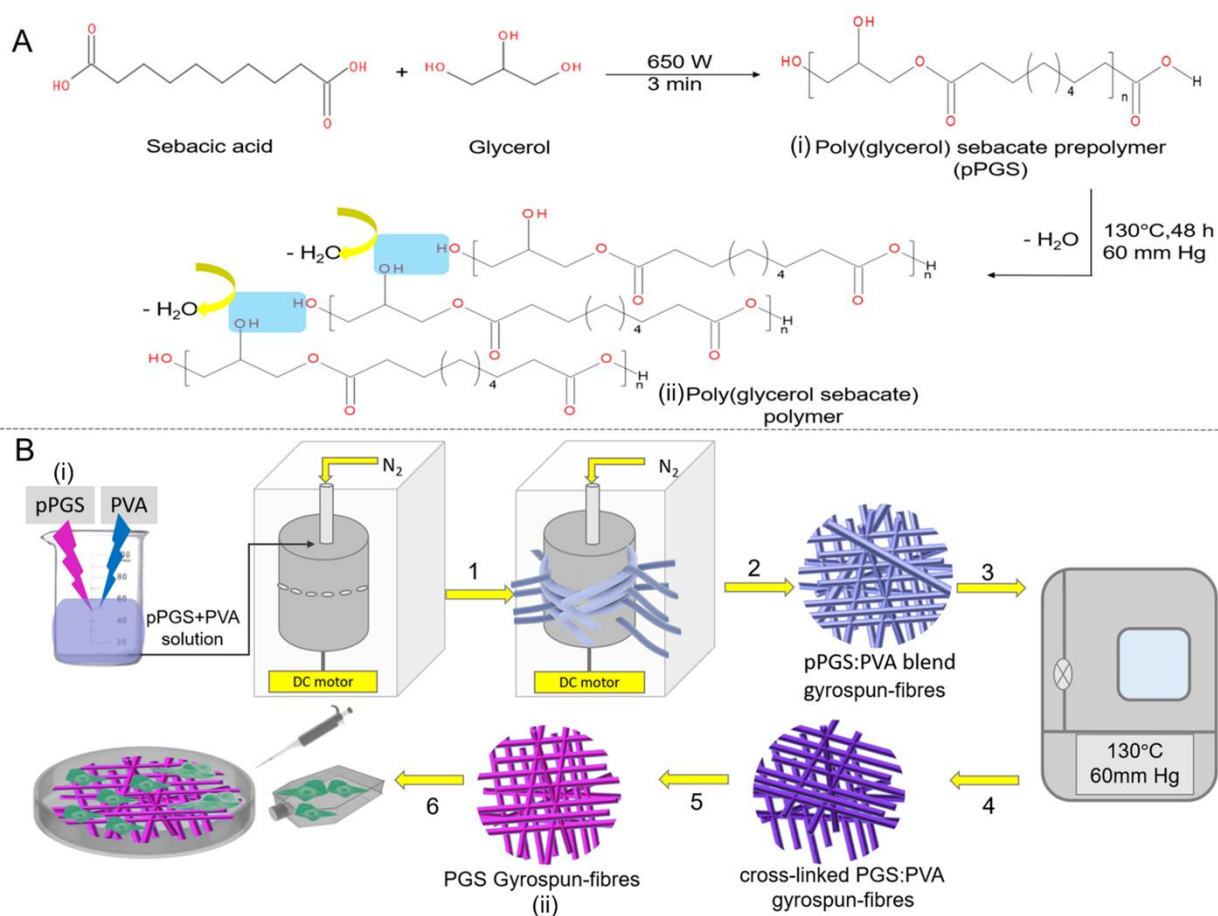


Figure 1: Schematic representation of A) PGS synthesis, B) Gyrospon fiber preparation and application steps 1. pressurized gyration, 2. collecting gyrospon fibers, 3. thermal crosslinking of PGS:PVA fibers, 4. collecting crosslinked fibers, 5. PVA removal, 6. evaluation of cell/fiber interaction.



## 2.6. Fiber Morphology

Gyrospon PGS fibers were evaluated by Scanning Electron Microscopy (SEM). Fiber samples were coated with a thin gold layer prior to SEM analysis (Q1500R ES, Quorum Technologies Ltd., UK). Fibers were studied both before and after cell culture. Fixation was performed prior to SEM analysis after cell culture studies. In the fixation process, the materials were washed with PBS and incubated in glutaraldehyde (2.5% (v/v)) solution for 30 min. Then, 15 min serial alcohol washes (25, 50, 70, 90, 95 and 100% (v/v)) and water contents of the cells were removed. In the last step, hexamethyl disilazane ( $\geq 99\%$ ) was added and the samples were allowed to dry. SEM analyses were performed with Hitachi (Japan) and TESCAN Gaia3 (Czech Republic) devices at an acceleration voltage of 5 kV.

## 2.7. Cell studies

Cytotoxicity of PGS polymer was tested in accordance with the standard ISO10993-5 "Biological evaluation of medical devices - Part 5, tests for *in vitro* cytotoxicity: Indirect MTT cytotoxicity" [31, 32]. Cytotoxicity tests were performed using the L929 (ATCC NCTC clone 929: CCL 1) mouse fibroblast cell line. Cells were incubated at 37 °C in >90% humidity and 5% CO<sub>2</sub> atmosphere within 90% DMEM, 10% FBS cultivation medium. Fibres were kept in the incubation medium with the 6 cm<sup>2</sup>/mL surface/medium ratio at 37 °C for 72 h. After 72 h, incubated medium extracts were interacted with the L929 cell lines in 96 well plates, overnight. Cell medium was used as a negative control and the 10% DMSO-90% cell medium mixture was used as a positive control. The day after, culture media were removed and cells interacted with 10% MTT ((4,5-Dimethylthiazol-2-yl)-2,5-diphenyltetrazolium bromide, 5 mg/mL) dye and 90% original

cell culture medium mixture at 37 °C for 4 h. After 4 h, the medium was replaced with 100µL propan-2-ol solution (with 0.04M HCl) and MTT dye dissolved. Then, absorbance of metabolised and dissolved MTT reagent was measured at 570 nm by ELISA micro plate reader and % cell viability values were obtained.

A fluorescent LIVE/DEAD™ Viability/Cytotoxicity Kit was used to examine the cell viability on the gyrospon PGS fibers. The Calcein AM cell dye contained in the kit gives the absorption in the 494/517 nm band by staining the living cells green, while the ethidium homodimer-1 cell dye staining the dead cells in red gives absorption in the 517/617 nm band [33]. For the examination of the cell-PGS gyrospon fibers interaction, fluorescent live/dead cell staining was performed up to 7 days of incubation. 100 µL of cell suspension (ATCC dermal fibroblast cells) at a concentration of  $1 \times 10^5$  cells/mL were seeded onto gyrospon fibers. 90% DMEM, 10% FBS, 4 mM L-glutamine, 100 IU/mL penicillin/streptomycin medium was used at 37 °C, 5% CO<sub>2</sub> and >90% humidity incubation conditions. 4 µM Ethidium homodimer-1 (EtdH-1) solution containing 2 µM Calcein AM was prepared in sterile PBS. At the end of 7 days, fluorescent live/dead cell staining were performed. After 45 min incubation, samples were washed with PBS and examined by fluorescence microscopy (Leica Microsystems, Germany).

### **3. Results and Discussion**

In this study, PGS prepolymers were synthesized from the glycerol and sebacic acid by microwave-assisted polymerization, then gyrospon fiber was produced from prepolymer using pressurized gyration and crosslinked. In order to obtain stable and uniform fibers, we optimized the key processing parameters such as molecular weight of polymer,

concentration of blended polymer solution, rotation speed, applied pressure and the results are discussed in the following sections.

$^1\text{H-NMR}$  spectrum of the synthesized pPGS is shown in the Figure 2A. The methylene peaks from the sebacic acid molecule were determined at  $\delta$ : 1.30, 1.62 and 2.35 ppm in accordance with the literature [29]. In addition, methylene peaks originating from glycerol were determined at  $\delta$ : 4.1-4.25 ppm and  $\delta$ : 5.3-5.4 ppm. Based on the NMR data obtained, it was confirmed that pPGS structures were synthesized successfully. The tetramethyl silane (TMS) was used as standard calibrating solvent.

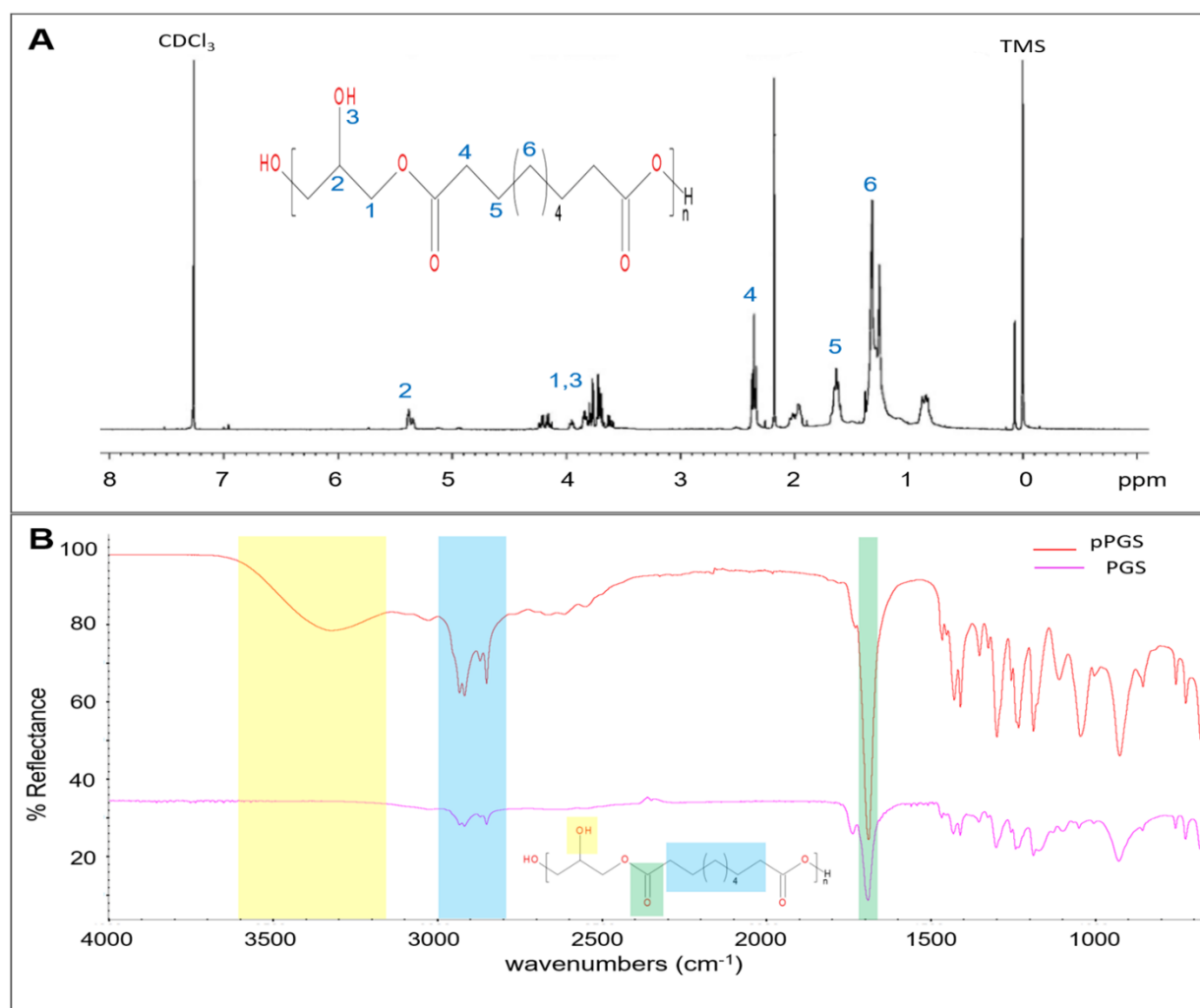


Figure 2: A) NMR spectrum of PGS prepolymer, B) FT-IR spectrum of pPGS and PGS polymers.

The chemistry of the PGS prepolymer and polymer investigated by FT-IR spectra is given in Figure 2B. PGS synthesis is based on the fact that the hydroxyl groups from the chemical structure of glycerol provide water elimination by covalent bonding with thermal effect. Therefore, the characteristic -OH stretching observed in the PGS prepolymer at the 3150-3600  $\text{cm}^{-1}$  wavelength band was lost in the PGS polymer. Infrared spectra showed that the -CH<sub>2</sub> vibration at the 2800-3000  $\text{cm}^{-1}$  band was confirmed and the sharp ester peak for C=O stretching was observed at 1730  $\text{cm}^{-1}$ , showing that synthesis of pPGS was performed successfully [34].

Thermal degradation of the synthesized pPGS and PGS polymer structures were determined by thermogravimetric analysis. The TGA thermograms of the pPGS and the PGS polymer structures are shown in Figure 3A. The thermal decomposition of the pPGS started at about 150 °C in the first step and the second decomposition was observed at 400 °C. PGS undergoes thermal degradation in a single step at about 420 °C. In the light of these data, it was observed that the prepolymer had two thermal degradation points depending on the sebacic acid and glycerol monomers, and the PGS polymer was obtained with high efficiency crosslinking, proved by a single thermal degradation point. DSC analyses were also performed to examine the thermal properties of the PGS polymer and to determine glass transition temperatures, which were given in Figure 3B. The glass transition temperature ( $T_g$ ) of PGS was determined as -28.3 °C which correlates well with literature [35, 36].

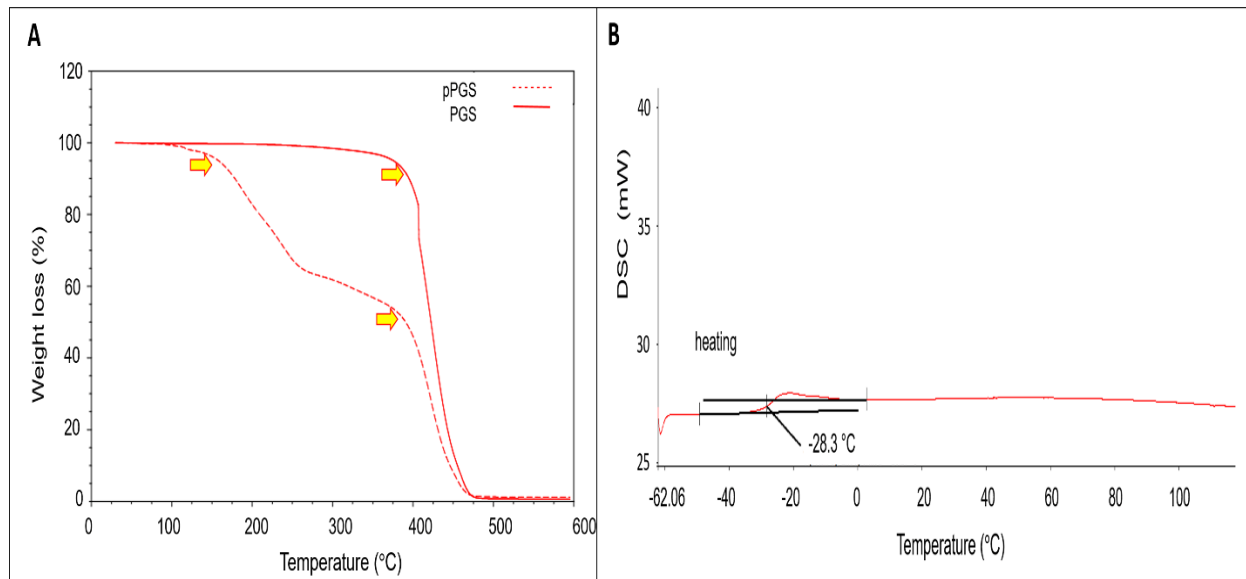


Figure 3: A) TGA thermograms of pPGS and PGS polymers, B) DSC thermogram of PGS polymer.

In terms of mechanical properties, there are several studies in the literature that the Young's modulus value of PGS varies between 0.05-1.50 MPa and it has a maximum elongation at break percentage between 40-500% depending on the crosslink temperature (120-150 °C), time (1 to 7 days) and mole ratio of sebacic acid to glycerol [37, 38]. In the present study, Young's modulus of PGS was found as  $0.21 \pm 0.02$  MPa and the maximum elongation at break was calculated as  $67 \pm 4.6\%$ . In the study conducted by Wang et al., the Young's modulus of PGS was reported as  $0.28 \pm 0.03$  MPa, the elongation at break was  $267 \pm 59.4\%$  and the tensile strength was 0.5 MPa [39]. In another study, Young's modulus of PGS was calculated as  $0.50 \pm 0.02$  MPa with 180% elongation at break for microwave induced synthesis and 150 °C, 16 h curing conditions [29]. Liu et al. also reported that the mechanical strength of PGS is changed by the monomer molar ratios and reaction conditions (temperature, curing time, pressure etc.) [40].

Considering the mechanical properties and the examples in the literature, it is interpreted that PGS can be used in soft tissue applications such as skin, muscle and ligament tissue engineering. Therefore, our aim was to form PGS polymers as fibrous scaffolds for potential soft tissue applications. In the recent years, pressurized gyration technique has become a novel and useful tool for scaffold fabrication without the need of electrical conductivity [41]. The main drawbacks of scaffold design with PGS are dissolution and fabrication problems of material. After crosslinking, it is not possible to dissolve and process PGS. The PGS based scaffolds can be fabricated from prepolymer but then it melts and loses its physical form during thermal crosslinking. The most widely used technique for PGS fabrication in the literature is salt leaching, but this method does not provide high interconnectivity for cell penetration [42-45].

To overcome the preparation disadvantages of PGS, blends could be formed with polymers which are soluble in a common solvent with PGS prepolymer, having a melting temperature above the crosslinking temperature and which can be removed from the structure after crosslinking [46]. A suitable polymer candidate to form blend solution with PGS prepolymer is PVA which meets these criteria and has been adapted to electrospin PGS [30, 47].

Pressurized gyration technique is a very appropriate method for scaffold design with PGS and its blended solutions. During the preparation of the gyrospun fibers, centrifugal force dominates in the preparation vessel which starts to rotate at high speed and the polymer solution contained therein begins to displace. At the same time, the pressure difference created by the applied pressure also exerts a force in which the polymer solution exits within the rotating container. Rotational force is the main factor for the polymer solution

to come out of the holes of the container. While the polymer jet in the holes is formed by the surface tension in the liquid-air interface, Marangoni stress caused by the liquid droplets and gas pressure interface triggers fiber jet formation [23, 26].

In addition, the collector distance and ambient conditions (temperature, humidity) are effective in fiber formation and morphology. Moisture imbalance/increase in ambient conditions negatively affects homogeneity of fiber morphology. Gyrospun fibers were obtained at  $45\pm 5\%$  humidity and  $24\pm 2$  °C temperature conditions during the study. The molecular weight, concentration, viscosity and volatility of the solvent (boiling point) of the polymer used in the prepared polymer-solvent system are the solution parameters that influence the fiber diameter. In the present study, PGS: PVA ratio (55:45) was kept constant and optimization studies were carried out by preparing polymer solutions at concentrations of 5, 10 and 15% (w/v) using different molecular weights of PVA.

The most important optimization parameter of pressurized gyration is the rotational speed. As the magnitude of the centrifugal force is exacerbated by increasing rotational speed, it leads to greater manipulation of the polymer solution and therefore leads to the formation of thinner fibers, which continuously prolong the polymer jet. For this purpose, we used the maximum rotation speed limit of system (36,000 rpm). At lower speeds jet formation was not observed as the force against the surface tension of the polymer was not overcome [19]. At low speeds, the polymer solution itself may diffuse from the polymer to the walls of the container due to its low surface tension.

The effect of gas pressure was examined as the second process control parameter affecting fiber formation. Because of the high volatility of HFIP (boiling point: 58.2 °C), when high pressure values were applied in the system (such as 0.2 and 0.3 MPa N<sub>2</sub>), no

fiber formed and the orifices of gyration holder blocked for each concentration of pPGS:PVA solutions. For optimum fiber formation, the gas pressure should be applied after reaching the critical rotational speed. If applied without reaching this value will cause evaporation of the solvent. After reaching the critical velocity, fiber morphology control can be provided by the gas pressure applied. The pressure difference between the inside and outside of the container increases the kinetic energy of the jet by applying an additional force to the polymer jet and allows it to extend further. The more elongated jet forms fibers with a smaller diameter and allows the solvent to evaporate faster [48]. When applied pressure was decreased to 0.1 MPa N<sub>2</sub>, fiber formation occurred in low molecular weight PVA blended with PGS prepolymer.

Fiber formation is not only dependent on pressure but also concentration of solution is an important parameter. Gyrospun fibers were not obtained from medium (pPGS:PVA<sub>M</sub>) and high (pPGS:PVA<sub>H</sub>) molecular weight PVA blended PGS prepolymer solutions at 10% and 15% (w/v) concentrations. Container orifices blocked and no fiber formation occurred. At lower concentrations (5% (w/v)) of pPGS:PVA<sub>M</sub> and pPGS:PVA<sub>H</sub> blend solutions, fiber formation was occurred with beaded and entangled fiber morphology. On the other hand, jet formation and fiber preparation could not be achieved at 5% (w/v) concentration of solutions using low (pPGS: PVA<sub>L</sub>) molecular weight PVA. Fiber formation was observed with bead formation at a concentration of 10 % (w/v) pPGS:PVA<sub>L</sub> (Figure 4A-B). Solvent evaporation is not fully achieved and bead formation was observed on the collecting elements by agglomeration of the solvent on the fibers.



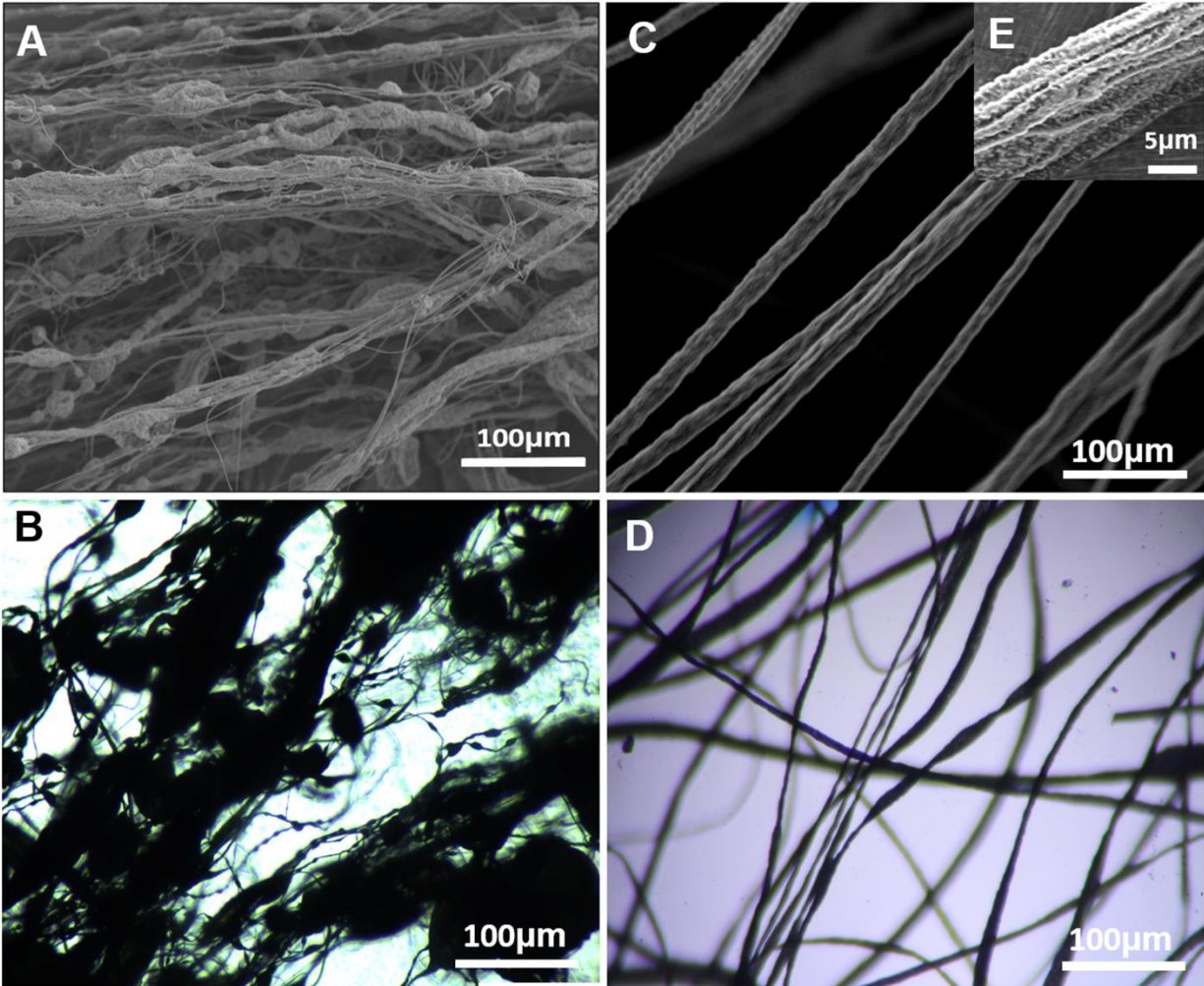


Figure 4: SEM and optical images of gyrospon fibers fabricated from A-B) 10 % (w/v) and C-D) 15 % (w/v) pPGS:PVAL blend solutions at 36,000rpm, 0.1MPa, respectively E) detailed SEM image of 15 % (w/v) pPGS:PVAL fibers.

Gyrospon fibers with smooth morphology were obtained at 15 % (w/v) concentration of pPGS:PVAL (Figure 4C-E). The viscosity of the 10% (w/v) pPGS:PVAL solution was found to be  $31.4 \pm 0.3$  mPa s and the solution of 15% (w/v) pPGS:PVAL was measured as  $90.2 \pm 0.4$  mPa s. It can be concluded that, increasing concentration and the related viscosity increase aids the formation of non-beaded fibers with smooth surface morphology. In addition, surface tension of the 10% (w/v) pPGS:PVAL solution was found

to be  $6.87 \pm 0.01$  mN/m and 15% (w/v) pPGS:PVAL was measured as  $6.55 \pm 0.04$  mN/m, respectively. The morphologies of the gyrospon PGS fiber structures were examined in terms of morphology and size (diameter) distribution after fabrication, crosslinking and PVA removal from the fibers (Fig. 5A-C). The average fiber diameters were measured as  $15.6 \pm 4.2$   $\mu\text{m}$  after pressurized gyration,  $15.8 \pm 3.1$   $\mu\text{m}$  after thermal crosslinking and  $11.8 \pm 2.9$   $\mu\text{m}$  after the PVA removal by washing procedure. There is no change in fibers average diameter after the thermal crosslinking step. However,  $\sim 25\%$  decrease was observed in the fibers diameter distribution after removal of PVA and unreacted PGS monomers/oligomers from the fiber structure by water and ethanol washes. In addition, fiber morphologies were flattened due to  $\text{H}_2\text{O}$  and PVA removal after thermal crosslinking and washing procedures respectively.

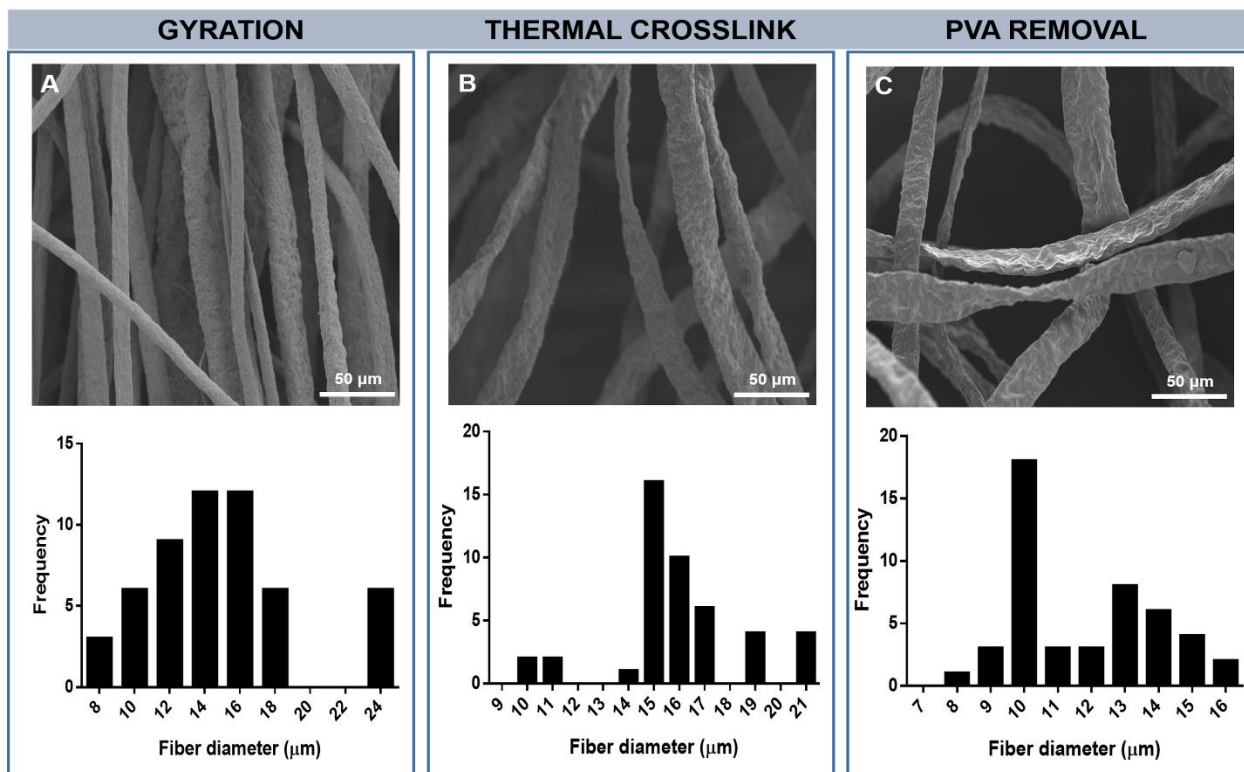


Figure 5: SEM images and the size distributions of gyrospon PGS:PVAL fibers after A) gyrosponing, B) thermal crosslinking and C) PVA removal.

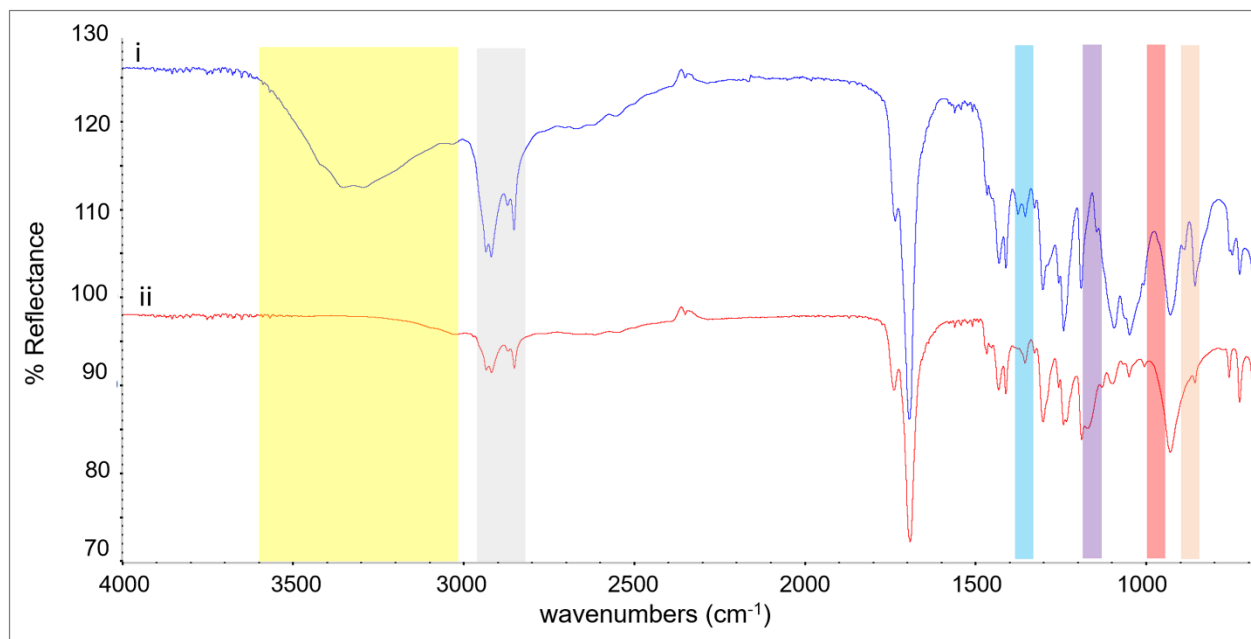


Figure 6: FT-IR spectra of (i) pPGS:PVAL gyrospon fibers, (ii) PGS gyrospon fibers after PVA removal.

The loss of -OH stretching peak at the 3150-3600  $\text{cm}^{-1}$  wavelength confirmed that PVA was washed away from the fiber structures and removed successfully [30]. In addition, it was observed that, the fiber morphologies were flattened after crosslinking and washing steps. PGS polymer (Figure 2) and PGS gyrospon fibers (after PVA removal) (Figure 6ii) showed the same characteristics for -OH stretching at the 3150-3600  $\text{cm}^{-1}$  wavelength band which was absent in the PGS polymer and the washed fibers. PVA removal from the fiber structure was investigated by evaluating the fingerprint region of FT-IR peaks of PVA. C-H bending at 1327  $\text{cm}^{-1}$ , C = O vibration in the 1240  $\text{cm}^{-1}$  band, the C-O stretching in the 1140, 920 and 843  $\text{cm}^{-1}$  bands, the C-C stretching in the 1240  $\text{cm}^{-1}$  band were also proved the PVA removal from the fiber structure.

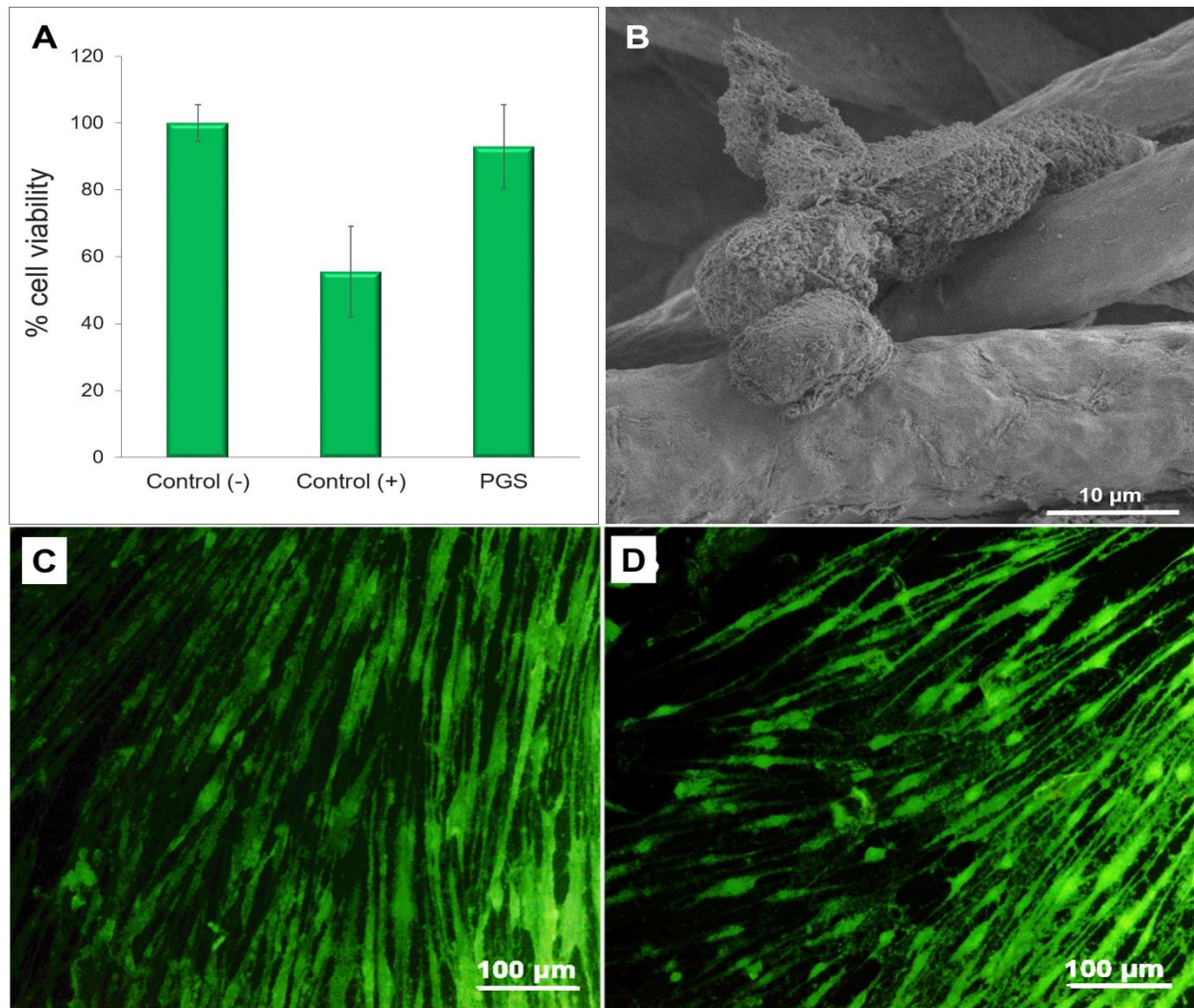


Figure 7: Cytocompatibility of PGS polymer and PGS gyrospon fibers. A) MTT cytotoxicity test result of PGS polymer, B) SEM image of PGS gyrospon fibers for 7day. Live/dead test fluorescent microscope images of C) TCP control, D) PGS gyrospon fibers for 7day.

Cells behaviours on PGS fibers are elucidated in Figures 7A-D. The MTT results showed that the synthesized PGS polymer has  $93 \pm 13\%$  cell viability (Figure 7A) without any toxic effect thanks to biocompatible and non-toxic monomers [49, 50]. Also, PGS fibers produced by the gyration technique exhibited superior cell viability and spreading on the gyrospon fibers without a toxic effect. It was observed that the dermal fibroblast cells are adhered to the gyrospon fiber surface and well-spread (Figure 7B). No cytotoxicity was

observed both in control and PGS gyrospon fibers for dermal fibroblast cells (Figure 7C and D). In a study conducted by Basnett et al. [51], poly(hydroxyalkanoate) gyrospon fibers and film surfaces were prepared and their cell interactions with the C2C12 myoblast and HMEC-1 microvascular endothelial cells was compared. It has been reported that, both of the cell types showed a statistically significant increase in terms of cell adhesion, proliferation and spreading on gyrospon poly(hydroxyalkanoate) elastomeric fibers compared to film surfaces. In our study, SEM images (Figure 7B) also indicates similar results. It is clear that adhered cell spread on the fibers and the cell-material interaction promotes cell hosting on the PGS fibers.

#### **4. Conclusions**

High preparation speed, ease of preparation and highly controlled fiber morphology are the hallmarks of pressurized gyration. In the present study; it has been concluded that the pressurized gyration is a suitable forming method for PGS fibers as scaffolds. Optimized pressure and rotation speed parameters allowed the preparation of PGS fibers with flat morphology and narrow size distribution. The resultant fiber structure provides 3D organization, allowing cells to infiltrate through the scaffold. Thus, in this article we have overcome the processability issues of PGS polymer which is a bioelastomer with excellent potential in tissue engineering applications.

#### **Acknowledgments**

This study is financially supported by Hacettepe University, Scientific Research Projects Coordination Unit (Grant No: TDK-2017-14725).

## Data availability

The raw/processed data required to reproduce these findings cannot be shared at this time as the data also forms part of an ongoing study.

## REFERENCES

- [1] D. Dippold, M. Tallawi, S. Tansaz, J. Roether, A. Boccaccini, Novel electrospun poly (glycerol sebacate)–zein fiber mats as candidate materials for cardiac tissue engineering, *European Polymer Journal* 75 (2016) 504-513.
- [2] J. Hu, D. Kai, H. Ye, L. Tian, X. Ding, S. Ramakrishna, X.J. Loh, Electrospinning of poly (glycerol sebacate)-based nanofibers for nerve tissue engineering, *Materials Science and Engineering: C* 70 (2017) 1089-1094.
- [3] D. Motlagh, J. Yang, K.Y. Lui, A.R. Webb, G.A. Ameer, Hemocompatibility evaluation of poly(glycerol-sebacate) in vitro for vascular tissue engineering, *Biomaterials* 27(24) (2006) 4315-24.
- [4] S. Salehi, T. Bahners, J. Gutmann, S.-L. Gao, E. Mäder, T. Fuchsluger, Characterization of structural, mechanical and nano-mechanical properties of electrospun PGS/PCL fibers, *RSC Advances* 4(33) (2014) 16951-16957.
- [5] S. Sant, D. Iyer, A.K. Gaharwar, A. Patel, A. Khademhosseini, Effect of biodegradation and de novo matrix synthesis on the mechanical properties of valvular interstitial cell-seeded polyglycerol sebacate–polycaprolactone scaffolds, *Acta Biomaterialia* 9(4) (2013) 5963-5973.
- [6] C.L. Nijst, J.P. Bruggeman, J.M. Karp, L. Ferreira, A. Zumbuehl, C.J. Bettinger, R. Langer, Synthesis and characterization of photocurable elastomers from poly (glycerol-co-sebacate), *Biomacromolecules* 8(10) (2007) 3067-3073.
- [7] R. Rai, M. Tallawi, A. Grigore, A.R. Boccaccini, Synthesis, properties and biomedical applications of poly (glycerol sebacate)(PGS): a review, *Progress in Polymer Science* 37(8) (2012) 1051-1078.
- [8] L. Liverani, A. Piegat, A. Niemczyk, M. El Fray, A.R. Boccaccini, Electrospun fibers of poly (butylene succinate–co–dilinoleic succinate) and its blend with poly (glycerol sebacate) for soft tissue engineering applications, *European Polymer Journal* 81 (2016) 295-306.
- [9] D. O'Brien, A. Hankins, N. Golestaneh, M. Paranjape, Highly aligned and geometrically structured poly(glycerol sebacate)-polyethylene oxide composite fiber matrices towards bioscaffolding applications, *Biomed. Microdevices* 21(3) (2019) 9.
- [10] P. Heydari, J. Varshosaz, A.Z. Kharazi, S. Karbasi, Preparation and evaluation of poly glycerol sebacate/poly hydroxy butyrate core-shell electrospun nanofibers with sequentially release of ciprofloxacin and simvastatin in wound dressings, *Polym. Adv. Technol.* 29(6) (2018) 1795-1803.
- [11] S. Sant, C.M. Hwang, S.H. Lee, A. Khademhosseini, Hybrid PGS-PCL microfibrinous scaffolds with improved mechanical and biological properties, *Journal Tissue Engineering and Regenerative Medicine* 5(4) (2011) 283-91.

- [12] N. Obregon, V. Agubra, M. Pokhrel, H. Campos, D. Flores, D. De la Garza, Y. Mao, J. Macossay, M. Alcoutlabi, Effect of Polymer Concentration, Rotational Speed, and Solvent Mixture on Fiber Formation Using Forcespinning®, *Fibers* 4(2) (2016).
- [13] R.T. Weitz, L. Harnau, S. Rauschenbach, M. Burghard, K. Kern, Polymer nanofibers via nozzle-free centrifugal spinning, *Nano letters* 8(4) (2008) 1187-91.
- [14] A.M. Loordhuswamy, V.R. Krishnaswamy, P.S. Korrapati, S. Thinakaran, G.D. Rengaswami, Fabrication of highly aligned fibrous scaffolds for tissue regeneration by centrifugal spinning technology, *Materials Science and Engineering: C* 42 (2014) 799-807.
- [15] S. Calamak, R. Shahbazi, I. Eroglu, M. Gultekinoglu, K. Ulubayram, An overview of nanofiber-based antibacterial drug design, *Expert Opinion on Drug Discovery* 12(4) (2017) 391-406.
- [16] C. Bayram, M. Demirbilek, E. Yalçın, M. Bozkurt, M. Doğan, E.B. Denkbaş, Osteoblast response on co-modified titanium surfaces via anodization and electrospinning, *Applied Surface Science* 288 (2014) 143-148.
- [17] U.S. Demir, R. Shahbazi, S. Calamak, S. Ozturk, M. Gultekinoglu, K. Ulubayram, Gold nano-decorated aligned polyurethane nanofibers for enhancement of neurite outgrowth and elongation, *Journal of Biomedical Materials Research Part A* 106(6) (2018) 1604-1613.
- [18] Y. Lu, J. Huang, G. Yu, R. Cardenas, S. Wei, E.K. Wujcik, Z. Guo, Nanobiotechnology, Coaxial electrospun fibers: applications in drug delivery and tissue engineering, *WIREs Nanomedicine and Nanobiotechnology* 8(5) (2016) 654-677.
- [19] P.L. Heseltine, J. Ahmed, M. Edirisinghe, Developments in Pressurized Gyration for the Mass Production of Polymeric Fibers, *Macromolecular Materials and Engineering* 303(9) (2018) 1800218.
- [20] S. Mahalingam, M. Edirisinghe, Forming of polymer nanofibers by a pressurised gyration process, *Macromolecular Rapid Communications* 34(14) (2013) 1134-9.
- [21] C. Bayram, Z. Ahmad, E.B. Denkbas, E. Stride, M.J. Edirisinghe, Electrohydrodynamic printing of silk fibroin, *Macromolecular Research* 21(4) (2013) 339-342.
- [22] S. Mahalingam, M. Meinders, M. Edirisinghe, Formation, stability, and mechanical properties of bovine serum albumin stabilized air bubbles produced using coaxial electrohydrodynamic atomization, *Langmuir* 30(23) (2014) 6694-6703.
- [23] S. Mahalingam, B.T. Raimi-Abraham, D.Q.M. Craig, M. Edirisinghe, Formation of Protein and Protein–Gold Nanoparticle Stabilized Microbubbles by Pressurized Gyration, *Langmuir* 31(2) (2015) 659-666.
- [24] F. Brako, R. Thorogate, S. Mahalingam, B. Raimi-Abraham, D.Q.M. Craig, M. Edirisinghe, Mucoadhesion of Progesterone-Loaded Drug Delivery Nanofiber Constructs, *ACS Applied Materials & Interfaces* 10(16) (2018) 13381-13389.
- [25] F. Brako, B.T. Raimi-Abraham, S. Mahalingam, D.Q.M. Craig, M. Edirisinghe, The development of progesterone-loaded nanofibers using pressurized gyration: A novel approach to vaginal delivery for the prevention of pre-term birth, *International Journal of Pharmaceutics* 540(1) (2018) 31-39.
- [26] S. Mahalingam, B.T. Raimi-Abraham, D.Q.M. Craig, M. Edirisinghe, Solubility–spinnability map and model for the preparation of fibres of polyethylene (terephthalate) using gyration and pressure, *Chemical Engineering Journal* 280 (2015) 344-353.
- [27] B.T. Raimi-Abraham, S. Mahalingam, M. Edirisinghe, D.Q.M. Craig, Generation of poly(N-vinylpyrrolidone) nanofibres using pressurised gyration, *Materials Science and Engineering: C* 39 (2014) 168-176.

- [28] F. Brako, B. Raimi-Abraham, S. Mahalingam, D.Q.M. Craig, M. Edirisinghe, Making nanofibres of mucoadhesive polymer blends for vaginal therapies, *European Polymer Journal* 70 (2015) 186-196.
- [29] H. Aydin, K. Salimi, Z. Rzayev, E. Pişkin, Microwave-assisted rapid synthesis of poly (glycerol-sebacate) elastomers, *Biomaterials Science* 1(5) (2013) 503-509.
- [30] E.M. Jeffries, R.A. Allen, J. Gao, M. Pesce, Y. Wang, Highly elastic and suturable electrospun poly(glycerol sebacate) fibrous scaffolds, *Acta Biomaterialia* 18 (2015) 30-9.
- [31] M. Gultekinoglu, Y.T. Sarisozen, C. Erdogdu, M. Sagiroglu, E.A. Aksoy, Y.J. Oh, P. Hinterdorfer, K. Ulubayram, Designing of dynamic polyethyleneimine (PEI) brushes on polyurethane (PU) ureteral stents to prevent infections, *Acta Biomaterialia* 21 (2015) 44-54.
- [32] J. Yun, J.S. Im, Y.-S. Lee, H.-I.J. Kim, Electro-responsive transdermal drug delivery behavior of PVA/PAA/MWCNT nanofibers, *European Polymer Journal* 47(10) (2011) 1893-1902.
- [33] E. Çelik, C. Bayram, R. Akçapınar, M. Türk, E.B. Denkbaz, The effect of calcium chloride concentration on alginate/Fmoc-diphenylalanine hydrogel networks, *Materials Science and Engineering: C* 66 (2016) 221-229.
- [34] Á. Conejero-García, H.R. Gimeno, Y.M. Sáez, G. Vilariño-Feltrer, I. Ortuño-Lizarán, A. Vallés-Lluch, Correlating synthesis parameters with physicochemical properties of poly (glycerol sebacate), *European Polymer Journal* 87 (2017) 406-419.
- [35] Q. Liu, M. Tian, R. Shi, L. Zhang, D. Chen, W. Tian, Structure and properties of thermoplastic poly(glycerol sebacate) elastomers originating from prepolymers with different molecular weights, *Journal of Applied Polymer Science* 104(2) (2007) 1131-1137.
- [36] B. Xu, Y. Li, C. Zhu, W.D. Cook, J. Forsythe, Q. Chen, Fabrication, mechanical properties and cytocompatibility of elastomeric nanofibrous mats of poly (glycerol sebacate), *European Polymer Journal* 64 (2015) 79-92.
- [37] Y. Li, W. Huang, W.D. Cook, Q. Chen, A comparative study on poly (xylitol sebacate) and poly (glycerol sebacate): mechanical properties, biodegradation and cytocompatibility, *Biomedical Materials* 8(3) (2013) 035006.
- [38] C.A. Sundback, J.Y. Shyu, Y. Wang, W.C. Faquin, R.S. Langer, J.P. Vacanti, T.A. Hadlock, Biocompatibility analysis of poly (glycerol sebacate) as a nerve guide material, *Biomaterials* 26(27) (2005) 5454-5464.
- [39] Y. Wang, G.A. Ameer, B.J. Sheppard, R. Langer, A tough biodegradable elastomer, *Nature Biotechnology* 20 (2002) 602.
- [40] Q. Liu, M. Tian, T. Ding, R. Shi, L. Zhang, Preparation and characterization of a biodegradable polyester elastomer with thermal processing abilities, *Journal of Applied Polymer Science* 98(5) (2005) 2033-2041.
- [41] H. Takahashi, K. Itoga, T. Shimizu, M. Yamato, T. Okano, Human neural tissue construct fabrication based on scaffold-free tissue engineering, *Advanced Healthcare Materials* 5(15) (2016) 1931-1938.
- [42] M. Souza, S. Tansaz, E. Zanotto, A. Boccaccini, Bioactive glass fiber-reinforced PGS matrix composites for cartilage regeneration, *Materials* 10(1) (2017) 83.
- [43] C.E. LeBlon, R. Pai, C.R. Fodor, A.S. Golding, J.P. Coulter, S.S. Jedlicka, In vitro comparative biodegradation analysis of salt-leached porous polymer scaffolds, *Journal of Applied Polymer Science* 128(5) (2013) 2701-2712.
- [44] K.-W. Lee, N.R. Johnson, J. Gao, Y. Wang, Human progenitor cell recruitment via SDF-1 $\alpha$  cocervate-laden PGS vascular grafts, *Biomaterials* 34(38) (2013) 9877-9885.



- [45] B. Xiao, W. Yang, D. Lei, J. Huang, Y. Yin, Y. Zhu, Z. You, F. Wang, S. Sun, PGS Scaffolds Promote the In Vivo Survival and Directional Differentiation of Bone Marrow Mesenchymal Stem Cells Restoring the Morphology and Function of Wounded Rat Uterus, *Advanced Healthcare Materials* (2019) 1801455.
- [46] M. Frydrych, B. Chen, Large three-dimensional poly (glycerol sebacate)-based scaffolds—a freeze-drying preparation approach, *Journal of Materials Chemistry B* 1(48) (2013) 6650-6661.
- [47] R. Khosravi, C.A. Best, R.A. Allen, C.E. Stowell, E. Onwuka, J.J. Zhuang, Y.-U. Lee, T. Yi, M.R. Bersi, T. Shinoka, Long-term functional efficacy of a novel electrospun poly (glycerol sebacate)-based arterial graft in mice, *Annals of Biomedical Engineering* 44(8) (2016) 2402-2416.
- [48] X. Hong, M. Edirisinghe, S. Mahalingam, Beads, beaded-fibres and fibres: Tailoring the morphology of poly(caprolactone) using pressurised gyration, *Materials Science and Engineering: C* 69 (2016) 1373-82.
- [49] Y. Jia, W. Wang, X. Zhou, W. Nie, L. Chen, C. He, Synthesis and characterization of poly (glycerol sebacate)-based elastomeric copolyesters for tissue engineering applications, *Polymer Chemistry* 7(14) (2016) 2553-2564.
- [50] X.J. Loh, A.A. Karim, C. Owh, Poly (glycerol sebacate) biomaterial: synthesis and biomedical applications, *Journal of Materials Chemistry B* 3(39) (2015) 7641-7652.
- [51] P. Bassett, S. Mahalingam, B. Lukasiewicz, S. Harding, M. Edirisinghe, I. Roy, Evaluation of porous polyhydroxyalkanoate (PHA) fibres as tissue engineering scaffold, *Front. Bioeng. Biotechnol.* (2016).

## GRAPHICAL ABSTRACT

